Dehazing redox homeostasis to foster purple bacteria biotechnology

Dehazing redox homeostasis to foster purple bacteria biotechnology

Abbas Alloul[1,*], Naïm Blansaer[1], Paloma Cabecas Segura[2], Ruddy Wattiez[2], Siegfried E. Vlaeminck[1], Baptiste Leroy[2]

[1] Research Group of Sustainable Energy, Air and Water Technology, Department of Bioscience Engineering, University of Antwerp, Antwerpen, Belgium

[2] Laboratory of Proteomics and Microbiology, University of Mons, Mons, Belgium

* Correspondence: Abbas.Alloul@UAntwerpen.be (A. Alloul)

[@]Twitter: A.A. @AbbasAlloul; N.B. @NBlansaer; S.E.V. @Siegfried_Vla

ORCID Authors: A.A. 0000-0003-4125-7470; N.B. 0000-0003-3974-7980; P.C.S. 0000-0002-9420-7058; R.W. 0000-0003-2071-4310; S.E.V. 0000-0002-2596-8857; B.L. 0000-0001-7166-4478

Abstract

Purple non-sulfur bacteria (PNSB) show great potential for environmental and industrial biotechnology, producing microbial protein, biohydrogen, polyhydroxyalkanoates (PHA), pigments, etc. Grown photoheterotrophically, the carbon source is typically more reduced than PNSB biomass, which leads to a redox imbalance. To mitigate the excess of electrons, PNSB can exhibit several 'electron sinking' strategies such as CO_2 fixation, N_2 fixation, H_2 and PHA production. The lack of a comprehensive (over)view of these redox strategies is hindering the implementation of PNSB for biotechnology applications. This review paper aims to present the state of the art of redox homeostasis in phototrophically grown PNSB, presenting known and theoretically expected strategies and discussing them from stoichiometric, thermodynamic, metabolic and economic points of view.

Keywords: purple phototrophic bacteria; alternative protein; polyhydroxybutyrate; resource recovery; hydrogen economy; nitrogen fixation

Glossary

- **Bacteriochlorophyll:** Pigment molecule located in the reaction center.
- **Carbon capture and utilization:** Processes focusing on the capture of CO_2 and reduction with H_2 or electricity to form high-value chemicals such as formate or methanol.
- **Electron sinking:** Mechanism or strategy to reoxidize metabolic cofactors, deal with the excess of electrons and maintain redox homeostasis.
- **Gibbs free energy:** Measure to define the thermodynamic equilibrium and direction of a reaction. Reactions with a positive change in Gibbs free energy (endergonic reactions) require external energy input and will not occur spontaneously in that direction, while reactions with a negative change in Gibbs free energy (exergonic reactions) will release energy and can occur spontaneously in that direction. Reactions are in equilibrium if the change in Gibbs free energy is equal to zero.
- **Membrane potential:** Charge gradient over the bacterial membrane and driving force for metabolic reactions such as ATP synthesis.
- **Microbial fertilizer:** The use of microbial biomass as organic fertilizer for plant growth.
- **Microbial protein:** The use of microbial biomass as protein ingredient for human food and animal feed applications.
- **Phototrophic growth:** Growth mode using light as energy source.
    - **Anoxygenic photosynthesis:** Phototrophic growth without oxygen production.
    - **Photoautotrophic growth:** Phototrophic growth with CO_2 as carbon source.
    - **Photoheterotrophic growth:** Phototrophic growth with organics as carbon and electron source simultaneously.
- **Proteobacteria:** A phylum of prokaryotes, mainly dominated by Gram-negative bacteria, covering a wide variety of morphologic and metabolic traits.
- **Reaction center:** Membrane-bound protein complex converting light energy into chemical energy through photooxidation and release of reduced electron transporters.
- **Redox homeostasis:** Maintenance of the oxidation degree of the cell interior milieu as opposed to the oxidation degree of the exterior environment.
- **Stoichiometry:** Quantitative association between substrates and formed products in a chemical reaction.
- **Thermodynamics:** Energetic relationship between substrates and formed products in a chemical reaction.

1 Redox homeostasis in phototrophically grown PNSB

Purple non-sulfur bacteria (PNSB), a group of microbes belonging to the alpha- and beta-**Proteobacteria**, have attracted the curiosity of microbiologists and engineers for decades due to their metabolic versatility and potential for synthesis of societal and economic relevant bioproducts [1]. There is a growing interest in implementing PNSB for environmental and industrial biotechnology applications such as wastewater treatment, bioremediation and production of **microbial protein**, **microbial fertilizer**, biohydrogen, bioplastics and pigments [2-6]. Especially for wastewater treatment, applications are accelerating these last five years with the construction of pilot and demo scale reactors in Australia [7], India (https://projectsaraswati2.com/) and Spain (https://deep-purple.eu/; https://incover-project.eu/). For biotechnology applications, PNSB are usually explored **photoheterotrophically** where they use light as energy source through **anoxygenic photosynthesis** and various organics such as volatile fatty acids (VFA), carbohydrates and amino acids as carbon and electron source [2,8-11]. As for all microbes, PNSB ought to maintain their internal **redox homeostasis** by balancing redox power-producing and consuming pathways. This is particularly challenging when PNSB grow **phototrophically** under anaerobic conditions on carbon sources more reduced than the biomass such as propionate, butyrate or longer chain VFA (Box 1).

Researchers discovered two main '**electron sinking'** strategies in PNSB to deal with this excess of redox power, namely CO_2 fixation through the Calvin cycle and H_2 production (Box 1, Figure I, Key Figure). More recently, several additional metabolic pathways were proposed that participate in redox homeostasis such as polyhydroxyalkanoate (PHA) or isoleucine production [12-14]. A fundamental understanding of redox homeostasis is essential for PNSB biotechnology because these 'electron sinking' strategies are often exploited to channel the excess of reducing power to the synthesis of biomass (proteins), PHA or H_2. Despite decades of research, a comprehensive (over)view of redox balancing strategies in phototrophic grown PNSB is missing. Key insights on redox homeostasis remain scattered and recent developments are not yet or only partly picked up by microbial biotechnologists. This review paper aims to present the state of the art of redox homeostasis in phototrophically grown PNSB, presenting known and theoretical strategies and discussing them from **stoichiometric**, **thermodynamic**, metabolic and economic points of view. This will help fundamental scientists

to better comprehend the metabolic maze of PNSB and assist applied researchers to pinpoint novel microbial control tools for the production of value-added bioproducts.

2 Stoichiometric and thermodynamic considerations of redox homeostasis

The established microbiology theoretical concepts to derive stoichiometries and thermodynamics are essential to acquiring a fundamental understanding of the catabolic and anabolic needs and products (Box 2). Element and electron balancing yields stoichiometry, and the bioenergetics allow judging whether biochemical reactions are possible in natural and engineered environments [15].

For phototrophically grown PNSB, the catabolism consists of anoxygenic photosynthesis generating the required energy, conserved in the form of ATP to drive the energy-consuming anabolic reaction. The stoichiometry reaction for growth reflects the anabolic substrates and products. The more positive the **Gibbs free energy** ΔG (endergonic), the higher the photosynthetic energy requirement (

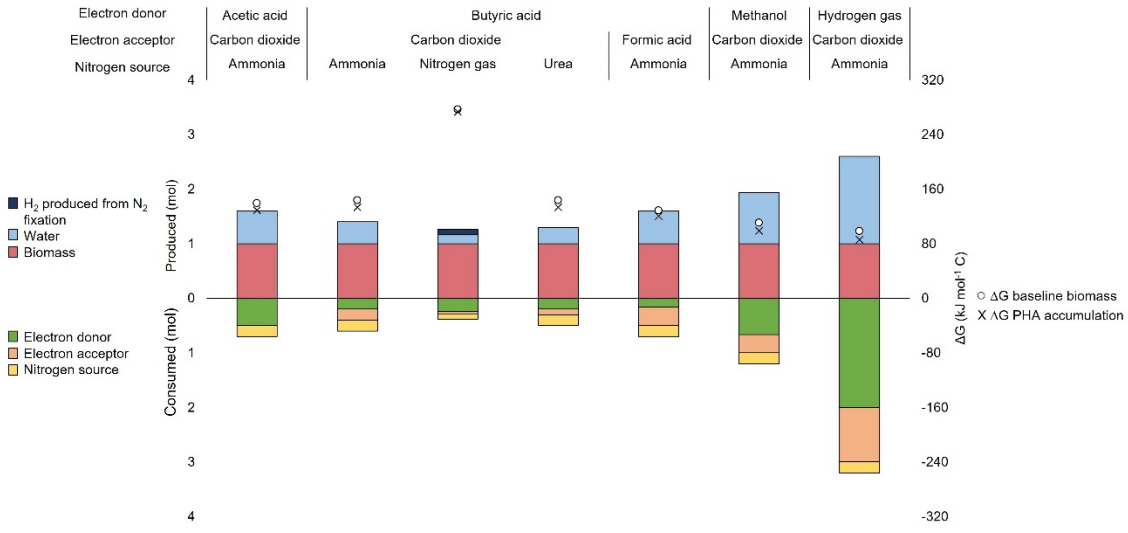

Figure *1*). Two main groups of electron sources are, currently, key in PNSB biotechnology: (i) VFA such as acetate, propionate and butyrate, for instance, generated through acidogenic fermentation of solid and liquid waste streams [16,17] and (ii) H_2 and C1 compounds derived from CO_2 reduction (e.g. formate and methanol), relevant in the context of the H_2 economy and **carbon capture and utilization** processes [18,19].

Balancing stoichiometries based on these industrially relevant electron donors yields several theoretical insights into electron balancing needs (

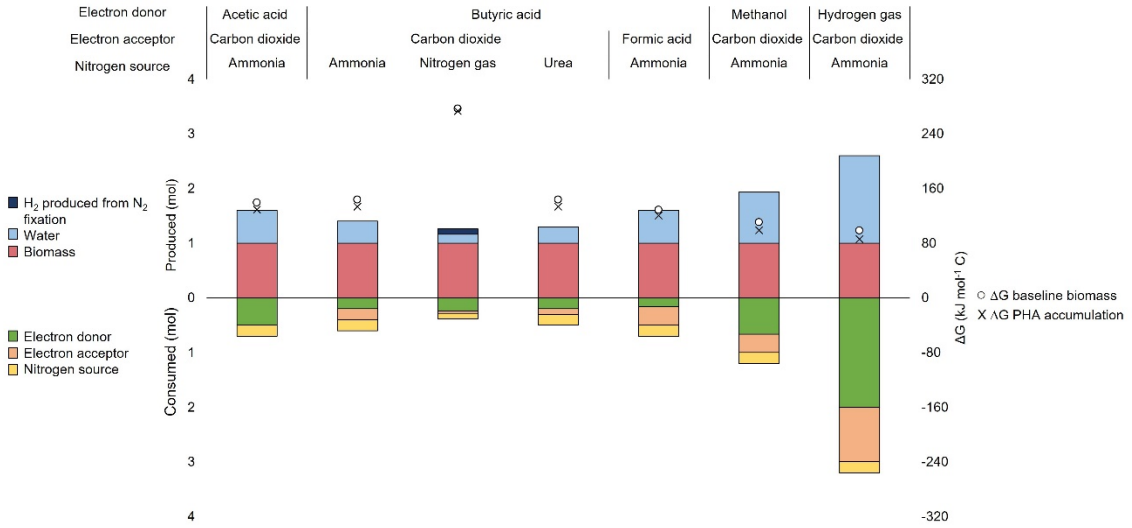

Figure ***1***). For VFA, growth of PNSB on acetate, for example, should theoretically not require CO_2 fixation through the Calvin cycle because the electron content is the same as for biomass (4 mol e^- mol^{-1} C; electron content relative to CO_2-C excl. PHA production; Box 1, Figure I). However, Laguna et al. [20] have shown that a *Rhodopseudomonas palustris* strain was unable to grow on acetate when the genes involved in the Calvin cycle were deleted. A similar observation was made for *Rhodospirillum rubrum*, which benefits from the presence of bicarbonate for phototrophic growth [21]. Cerruti et al. [22], on the other hand, observed a net CO_2 production for a *Rps. palustris* strain grown on acetate. Different elemental compositions and, thus, different biomass electron contents might explain this discrepancy of CO_2 fixation vs. production. For *Rs. rubrum,* a lower biomass electron content compared to acetate has been reported (3.7-4.2 vs. 4.0 mol e^- mol^{-1} $C_{biomass}$; Box 1, Figure I) [23]. Growth of *Rs. rubrum* on acetate would, therefore, require some degree of redox balancing.

Developments in carbon capture and utilization processes will open new routes for the production of building blocks such as methanol and formate for the chemical industry and biotechnology [18,24,25]. Photoassimilation of these carbon sources has been observed for several PNSB such as *Rhodobacter sphaeroides*, *Rps. palustris* and *Rps. acidophila* [26-28]. From a metabolic perspective, methanol is first converted to formate through a cascade of enzymes including methanol dehydrogenase, formaldehyde dehydrogenase and S-formylglutathione hydrolase [27]. For each mole of methanol, 2 moles NAD(P)H are generated. To assimilate the carbon to biomass, formate is eventually converted to CO_2 through the enzyme formate dehydrogenase generating an additional amount of 2 moles NAD(P)H. The CO_2 is finally fixated through the Calvin cycle using 4 moles NAD(P)H. For formate, however,

a net input of NAD(P)H is required because the Calvin cycle requires more NAD(P)H than generated from the oxidation of formate. Formate will, therefore, act as an electron acceptor for phototrophic growth on reduced carbon sources. Compared to CO_2, formate can be considered a less efficient electron acceptor because it contains a higher amount of electrons (Box 1, Figure I). More moles of formate are, therefore, required per mole carbon assimilated compared to CO_2.

The nitrogen source seems to have an important role in redox homeostasis as it can also be an electron carrier (

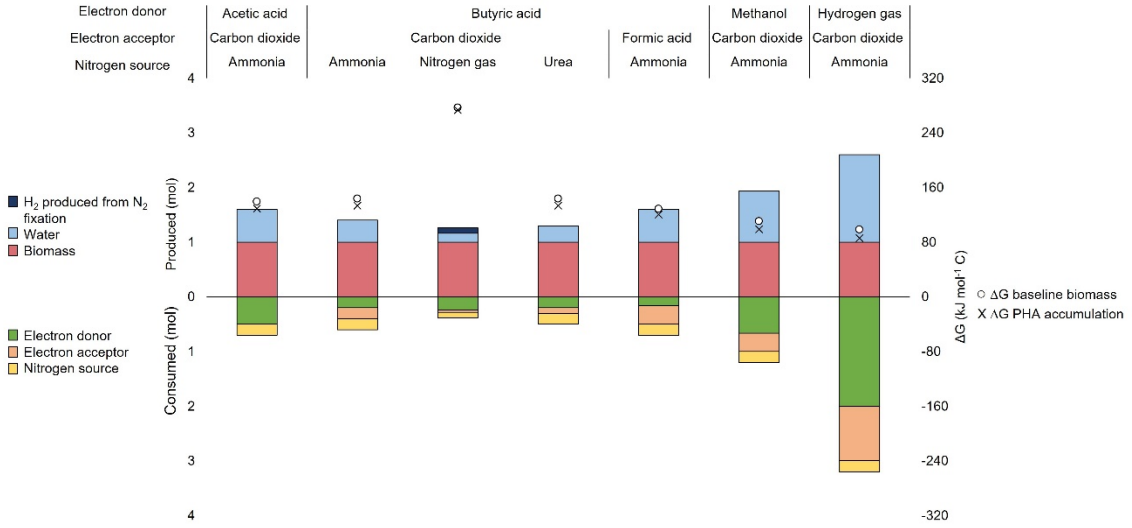

Figure ***1***). N_2 fixation, a common metabolic trait of PNSB, will decrease the CO_2 fixation requirement because the nitrogenase enzyme consumes electrons (8 mol e^- mol^{-1} N_2 fixed). This is also true if urea (0 mol e^- mol^{-1} N; Box 1, Figure I) is used as a nitrogen source, only requiring 0.1 mol CO_2 mol^{-1} $C_{biomass}$ for photoheterotrophic growth on butyrate (excl. PHA or H_2 production). External CO_2 requirements are probably lower because hydrolysis of urea releases one mole of CO_2. Equal amounts of CO_2 will, hence, be fixed during growth on urea as would be required for photoheterotrophic growth on NH_3.

In terms of thermodynamics, all anabolic reactions on NH_3 and organics require roughly the same photosynthetic energy regardless of the electron donor or acceptor (98-144 kJ mol^{-1}

$C_{biomass}$;

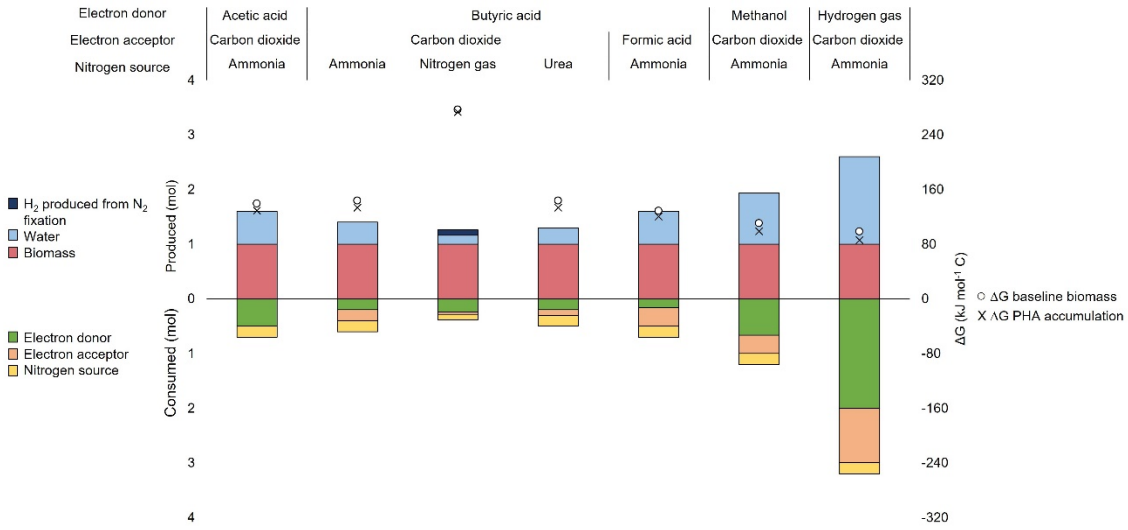

Figure *1*). There is, however, a great discrepancy in energy need compared to phototrophic growth on N_2 (274 kJ mol^{-1} $C_{biomass}$). N_2 fixation is an energy-intensive pathway, which requires 8 moles of ATP per mole N assimilated for molybdenum nitrogenase [29]. The thermodynamic advantage of the Calvin cycle is probably the reason why it is favored as redox balancing mechanism over N_2 fixation combined with H_2 production. Recently, H_2 production for phototrophic growth of *Rs. rubrum* on a mixture of butyrate and propionate in the presence of NH_3 was observed [30]. The nitrogenase enzyme can also, in the absence of N_2 and NH_3, channel all electrons to H_2 production without N_2 fixation. This is typically performed by sparging photobioreactors with argon [29]. Photoheterotrophic growth on NH_3 as nitrogen source and butyrate as carbon source, using a hydrogenase enzyme to dump excess reducing power, would require 155 kJ mol^{-1} $C_{biomass}$. This is thermodynamically more appealing than the N_2 fixation route, yet less energy efficient compared to the Calvin cycle. Thermodynamics fall short to clarify the observed H_2 production in the presence of NH_3 and there is, thus far no metabolic explanation (section 3.1).

Next to CO_2 fixation and H_2 production, PNSB can also accumulate PHA as carbon and energy storage. PHA accumulation is, from a thermodynamic perspective, slightly more appealing as redox balancing mechanism compared to CO_2 fixation (86-133 vs. 98-144 kJ mol^{-1} $C_{biomass}$). It can, therefore, be anticipated that PNSB shift towards a combination of CO_2 fixation and PHA accumulation when conditions are favorable (e.g. carbon source preferably VFA, high carbon to nitrogen ratios and high light intensity) [31]. This 'hierarchy' in redox balancing was also observed by Cerruti et al. [22], showing that the electrons first flow to CO_2 fixation and PHA production and only secondary to H_2 production when PHA storage is saturated. These experiments were performed with continuous illumination and with light-dark

cycles. Constant CO_2 production of 0.075 mmol h^{-1} was observed during continuous illumination. During light-dark cycles, CO_2 peaks appeared. Only minor levels of H_2 were produced (0.025 mmol h^{-1}). Cerruti et al. [22], therefore, concluded that H_2 production did not play a major role in redox homeostasis for their experiments.

Overall, the thermodynamic analysis helps to understand which redox balancing strategy is more appealing from an energy perspective (lowest ΔG). Even for the photoheterotrophic PNSB that generate their energy from cyclic photophosphorylation (BOX 1), light can be limiting and, thus, metabolic choices need to be made to balance energy production, consumption and redox stress. These choices in terms of redox strategies are partially regulated by gene expression. Masepohl [32] has written an extensive review on the regulation of N_2 fixation for *Rs. rubrum*, *Rps. palustris* and *Rb. capsulatus*. N_2 fixation apparently responds to NH_3, oxygen, light, molybdenum and iron. For *Rb. capsulatus*, for example, in the absence of NH_3, the NtrC protein is phosphorylated which then activates the expression of the nifA genes leading to N_2 fixation through molybdene nitrogenase activity. An increase in NH_3 results in dephosphorylation of the NtrC protein and inhibition of the NifA proteins. Oxygen also influences N_2 fixation by inhibiting nitrogenase activity.

3 Metabolic considerations of redox homeostasis

3.1 Key redox strategies for phototrophic growth on volatile fatty acids

Since the first scientific discovery of PNSB in 1931, no systematic overview of redox homeostasis has been described thus far [33]. In the following section, five key 'electron sinking' strategies essential for the phototrophic growth of PNSB are proposed.

The role of the Calvin cycle as redox balancing mechanism in PNSB has been well established by using mutants deleted of key enzymes (e.g. RuBisCO or phosphoribulokinase) [34,35]. The Calvin cycle is effective in reoxidizing the reduced cofactors because the fixation of one mole CO_2 oxidizes two moles of NADPH (Figure 2). In terms of energy use, the Calvin cycle consumes three moles of ATP per fixed CO_2. For VFA assimilation, alternative carbon fixation routes have been observed in PNSB namely, the ethylmalonyl-CoA pathway and reverse tricarboxylic acid pathway. Researchers demonstrated that the ethylmalonyl-CoA pathway is mainly used in PNSB during acetate and butyrate assimilation [21,36,37]. When using the ethylmalonyl-CoA pathway for acetate assimilation to 2-oxoglutarate, two moles CO_2 are fixed for every ATP consumed (Figure 2). Ethylmalonyl-CoA based acetate assimilation also results in the reoxidation of four reduced cofactors. In terms of redox balancing strategies,

the Calvin cycle is, thus, more efficient than the ethylmalonyl-CoA, yet the latter consumes lower levels of ATP. Some PNSB possess a functional glyoxylate shunt which is used for acetate assimilation. In this case, assimilation of two moles acetate and one mole CO_2 to 2-oxoglutarate does not lead to the reoxidation of reduced cofactors (Figure 2). PNSB species that use the glyoxylate shunt for acetate assimilation, therefore, require a functional Calvin cycle for carbon assimilation. Species that do not possess a functional glyoxylate shunt rely on ethylmalonyl-CoA for acetate assimilation and, therefore, do not require the Calvin cycle for redox balancing [20,38,39].

H_2 production, another key redox sink for phototrophically grown PNSB, is generated by the activity of two types of enzymes namely hydrogenase and nitrogenase. Hydrogenase can either produce or consume hydrogen gas, while nitrogenase can only produce hydrogen gas [29]. Nitrogenase derepression was observed in RuBisCO mutants of *Rs. rubrum* and *Rb. sphaeroides*, even in the presence of NH_3, probably through regB gene activity [40,41].

More recently, PHA production was proposed to serve as an 'electron sinking' mechanism, in addition to its more typical function as carbon storage [13,14,42,43]. From acetate, the production of PHA effectively conduces to the reoxidation of cofactors which could help cells deal with redox imbalance (Figure 2) [13,44]. This is, however, only transiently since stored PHA are always reconsumed when the carbon source is limiting [31]. When propionate or butyrate are assimilated, PHA synthesis does not act anymore as 'electron sinking' mechanism because no cofactor can be reoxidized during their synthesis (Figure 2). This is in agreement with our observation for *Rs. rubrum*. Only acetate triggered high-level PHA production, which was negatively influenced by the presence of bicarbonate [21,30,45-47]. A sudden increase in light intensity, which also results in redox imbalance (Box 3), has been shown to trigger PHA production [13], thereby, reinforcing the role of PHA in transient redox balancing.

Just recently, it was observed that proteins from the branched-chain amino acid synthesis and degradation pathways were often upregulated during VFA assimilation [9,13,21]. This new pathway could indeed represent an assimilation route converting acetyl-CoA to propionyl-CoA and then 2-oxoglutarate. The rationale for the existence of such an alternative assimilation route remains, however, unclear. The level of intracellular isoleucine was subsequently observed to be significantly higher in conditions that trigger redox imbalance in *Rs. rubrum*. Inhibiting the isoleucine synthesis by adding this amino acid to the environment also delayed the growth of *Rs. rubrum* on acetate [12]. From three moles of acetyl-CoA, the production of one mole of isoleucine allows the reoxidation of two reduced cofactors (Figure

2). Accumulation of isoleucine, could thus also be a way for *Rs. rubrum* to cope with redox stress. Accumulation of isoleucine was also observed in response to light-induced redox stress (Box 3). This newly proposed 'electron sinking' mechanism still requires definitive demonstration (see Outstanding Questions).

The reverse tricarboxylic acid pathway could also be used by bacteria as an 'electron-sinking' pathway for alpha-ketoglutarate production and its derived amino acid (Figure 2) [42,48]. McCully et al. [49] recently demonstrated that the flux through the reverse tricarboxylic acid pathway increased in a Calvin cycle mutant strain of *Rs. rubrum,* suggesting its involvement in redox balancing. Such a compensatory mechanism is dependent on the presence of adequate enzymes allowing fumarate reduction and reductive alpha-ketoglutarate synthesis which is apparently not possible for all PNSB and notably not in *Rp. palustris*.

Auxiliary oxidants (e.g. trimethylamine N-oxide, dimethyl sulfoxide, sulfate, nitrate) are also known electron acceptors that allow PNSB to reach redox homeostasis through anaerobic respiration [50,51]. Formation of hydrogen sulfide from sulfate is also an alternative respiratory mechanism for 'electron sinking', yet it is apparently not used as a compensatory route in a Calvin cycle mutant strain of *Rs. rubrum* [49] [52]. Nitrate respiration to nitrite can also be performed by PNSB that possess a dissimilatory nitrate reductase. Interestingly, *Rb. sphaeroides* possesses two different Nap-type nitrate reductases [53], one being specifically expressed under low oxygen levels which can thus also fulfill the role of 'electron sinking' in the presence of nitrate.

Next to phototrophy on VFA, some PNSB species such as *Rb. sphaeroides* are also able to use methanol [27]. This carbon source has a high electron content (6 mol e^- mol^{-1} C; Box 1, Figure I) and will, therefore, impose high levels of redox stress in phototrophically grown PNSB. Thus far, research on the growth of PNSB on methanol is limited to studies from the 70s merely focusing on initial screening and growth characterization [28,54,55]. Redox homeostasis strategies for methanol have never been described, yet are crucial with regards to the developments in carbon capture and utilization processes [25].

3.2 Complexity to elucidate: Mixed electron sources and open cultures

For the photoassimilation of VFA, only CO_2 fixation and H_2 production have been analyzed to some extent. The role played by anaerobic respiration and PHA or isoleucine synthesis in a biotechnological relevant context still requires detailed analysis. An even greater knowledge gap exists for growth on VFA mixtures, conditions more likely in natural and engineered systems. Recently, it was observed that *Rs. rubrum* does not rely on bicarbonate

supplementation when a mixture of butyrate and propionate is supplied. Instead of using the Calvin cycle for CO_2 fixation, *Rs. rubrum* turns to H_2 production [30]. Cultures growing on VFA mixtures also perform better in terms of growth and resistance to redox stress [17,56], yet how redox balancing is regulated remains largely unclear.

Differences in redox balancing strategies also exist between PNSB species. In terms of carbon assimilation efficiency, for instance, variation was observed for different strains [17]. The genetic background also influences how PNSB respond to different carbon and electron contexts [42,49] and notably the presence of a functional glyoxylate shunt is of major importance for 'electron sinking' (Figure 2). This was demonstrated by Shimizu et al. [38] who successfully increased H_2 production in *Rb. sphaeroides* by genetically introducing a functional glyoxylate shunt.

Next to the five key 'electron sinking' strategies (section 3.1), differences in redox balancing might also arise due to the particular enzyme deployed. For N_2 fixation, for example, three structurally and phylogenetically isoforms exist namely, molybdenum, iron and vanadium nitrogenase [57]. Luxem et al. [58] have shown for a *Rps. palustris* strain that these nitrogenases have different H_2 production to N_2 fixation ratios, ranging from 0.9-1.4 mol H_2 mol^{-1} N_2 for molybdenum nitrogenase and 3.9-6.9 mol H_2 mol^{-1} N_2 for iron nitrogenase. The extensive allocation of electrons to H_2 for each N_2 fixated in the iron nitrogenase strain eventually leads to slower growth [58]. Additional research is required to elucidate whether enzyme isoforms play a role in other redox pathways.

Next to experimental research, valuable insight on redox strategies can also be extrapolated from genome-scale metabolic models and metabolic and expression models. These models are a mathematical description of known metabolic pathways encoded in the organism's genome with or without cellular expression [59]. Chowdhury et al. [60], for example, predicted that malate dehydrogenase and 3 phosphate dehydrogenase are essential to maintain redox homeostasis in a *Rps. palustris* strain next to the Calvin cycle. Another metabolic model for *Rps. palustris* predicted that the oxidation state of the quinone pool relates to the CO_2 fixation rate, as the accumulation of reduced quinols will limit the electron flow and ATP generation for the Calvin cycle [61]. A recent study by the same authors indicated that high molecular weight and reduced carbon sources result in excess production of carbon and NAD(P)H, which can be channeled to PHA production Alsiyabi et al. [62].

4 Economic considerations

In biotechnology, the redox balancing strategies described in previous sections are often exploited to boost the flow of the excess of electrons to the synthesis of biomass (proteins), PHA or H_2. In this section, a cost estimation of the main feedstocks allows assessing the viability of several options for industrial biotechnology. This main feedstocks-based cost estimation is a considerable fraction of the overall operational expenditure. It accounts for the electron donor/acceptor and nitrogen source (Figure 3). It can, therefore, be anticipated that the market price of the bioproduct, estimated as three times the main feedstock cost, ought to be lower than the market price of their conventional alternatives. The particular bioprocess will, otherwise, not be economically viable.

For PNSB applications as food or feed ingredient, a.k.a. microbial protein, surplus redox power should mainly flow to microbial biomass (and hence protein). Replacing fishmeal in aquaculture with protein-rich PNSB biomass [3,63] appears to be interesting for several biotechnology routes as the selling price is comparable (Figure 3). Substituting soybean, on the other hand, typically used as a feed ingredient for cattle and poultry, will not be sustainable from an economic perspective. In terms of electron donor, growth on methanol appears to be the most appealing route for microbial protein production. Research, however, on methanol and C1-compounds is limited (section 3.1). Current developments in carbon capture and utilization processes will probably make CO_2-derived methanol more interesting for PNSB production in future research and applications [18,25]. In terms of VFA, only acetate shows to be attractive (€474-947 ton^{-1} biomass). Production of PNSB biomass on recovered VFA from fermented waste streams may be more appealing than using synthetic VFA [16,17]. This would avoid the cost of the electron donor and acceptor, yet might introduce new challenges such as microbial selectivity for high PNSB abundance and stability in nutritional quality [17,64]. Next to heterotrophy, PNSB are also able to grow **photoautotrophically** on H_2 and CO_2 as electron donor and acceptor, respectively [19]. From a purely economic perspective, however, photoautotrophic microbial protein production will be challenging as costs for the electron acceptor are high because it is the only carbon source for the cell (€300-510 ton^{-1} CO_2) [65,66]. Cultivation of PNSB as an added-value food ingredient might be more fit for this route, especially with the growing interest in the H_2 economy [25].

Next to microbial protein, PNSB are also explored for PHA and H_2 production. Based on the main feedstock cost estimation, particularly PHA shows to be interesting. PHA production will result in a slight increase in cost relative to microbial protein production, yet

this will be offset by the higher market price of the commodity (€3,500-5,340 ton^{-1} PHA) [67]. For H_2 production, waste streams are typically targeted because the market value of H_2 as energy source is too low (€1300-1900 ton^{-1} H_2) to even cover the feedstock costs [68].

5 Concluding remarks and future perspectives

Since the discovery of PNSB 91 years ago, they have predominantly been studied from a microbiological perspective. Last years, however, there is a growing trend in implementing PNSB for environmental and industrial biotechnology. Redox balancing is central here because researchers and engineers aim to maximize the excess of electrons to the synthesis of PNSB bioproducts. This paper is the first initiative to present a comprehensive (over)view of redox homeostasis in phototrophically grown PNSB. From a stoichiometric perspective, we could partly explain how differences in 'electron sinking' requirements occur for different carbon and nitrogen sources. Growth on acetate and urea, for example, reduces redox stress for PNSB relatively to butyrate or NH_3. Thermodynamics predict a 'hierarchy' in redox strategies. 'Electron sinking' through CO_2 fixation and PHA accumulation is energetically more favorable compared to H_2 production. From a metabolic perspective, several key redox strategies exist in phototrophically grown PNSB namely, CO_2 fixation, PHA accumulation, H_2 and alpha-ketoglutarate production and potentially intracellular isoleucine accumulation. Finally, the economic feedstock estimation highlights opportunities for methanol and VFA as electron donor for industrial biotechnology applications.

Future researchers should, first of all, focus on elucidating the 'hierarchy' in redox balancing. This 'hierarchy' has been observed for a *Rps. palustris* strain [22], yet additional research should confirm whether it is a general trait for PNSB (see Outstanding Questions). Dedicated research initiatives on redox homeostasis are, therefore, necessary with a complete characterization of the 'electron sinking' routes (i.e. CO_2, PHA, H_2 and isoleucine). How PNSB deal with redox homeostasis when multiple carbon and electron sources are present remains largely unexplored, even though this situation would be closer to natural and engineered environments. The number of PNSB species studied should be expanded and the respective gene clusters involved should also be characterized. This will allow for rapid *in-silico* testing of the genetic capacity for certain redox strategies through genome mining (section 3.2). Redox homeostasis in mixed cultures should also be studied because in natural and engineered environments PNSB thrive in open communities with other (non-)PNSB species. First, it should be explored whether there exists a kind of specialization in open PNSB cultures supplied with mixtures of electron sources. PNSB communities may, for example, exhibit division of labor, with PNSB species using different electron sources. Secondly, natural ecosystems and photobioreactors are not continuously illuminated or anaerobic, triggering (an)aerobic

chemotrophy next to the central phototrophic metabolism. These potential shifts from photosynthetic redox balancing to oxygen-driven 'electron sinking' need to be elucidated. The next step for the economics requires a full cost assessment, taking capital and operational expenditure into account as well as uncertainty. Dedicated life cycle assessment can support the economic insights and help direct researchers to target the most sustainable and opportune electron donors for the production of PNSB products.

Acknowledgments

This study was supported by the Concerted Research Action (ARC) project "PHASYN". Work of B. L. was supported by CDR funding "Redox homeostasis in purple bacteria" (CDR FRS-FNRS). The authors kindly acknowledge the Research Foundation - Flanders (FWO) for supporting A.A. with a postdoctoral fellowship (12W0522N); the project PurpleRace (40207) funded by the Industrial Research Fund (IOF) from the University of Antwerp for financial support of A.A. and N.B.

Figure legends

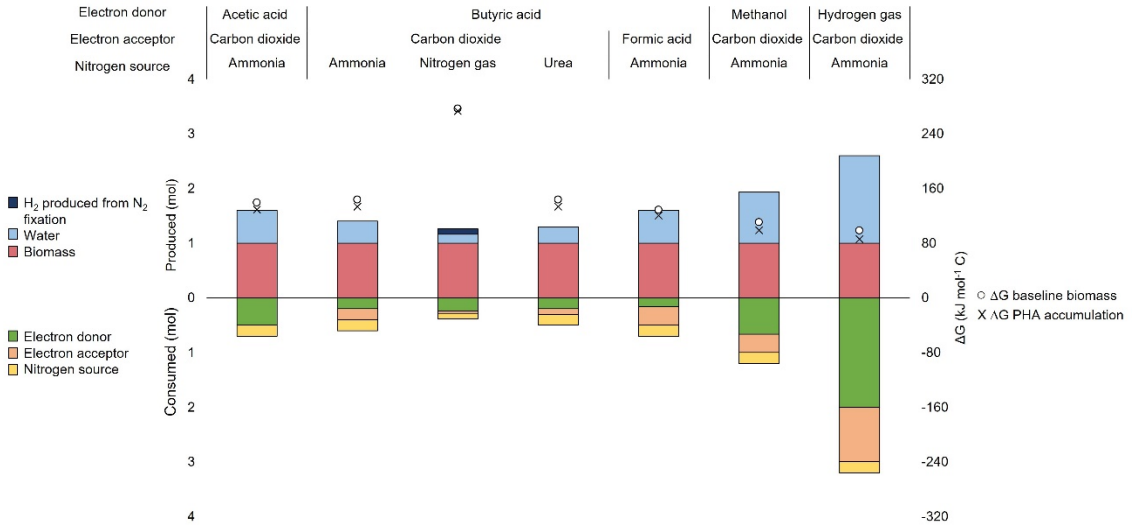

Figure 1 Stoichiometry and thermodynamics for phototrophically grown purple bacteria Theoretical stoichiometry on a molar basis (left y-axis) and associated Gibbs free energy requirements (right y-axis) for phototrophically grown purple bacteria on four electron donors, two electron acceptors and three nitrogen sources. For the stoichiometry, one scenario is shown based on biomass ($C_5H_7O_2N$) production excluding polyhydroxyalkanoates (PHA). Two Gibbs free energy scenarios were simulated: (i) biomass production without PHA, and (ii) biomass production including 20% of the electrons stored as PHA. PHA was composed of 50% polyhydroxybutryate ($C_4H_6O_2$) and 50% polyhydroxyvalerate ($C_5H_8O_2$). Stoichiometries and associated Gibbs free energy values were calculated according to methodologies and values from *Kleerebezem and Van Loosdrecht [15]* and Metcalf et al. [69], respectively (pH 7 and 25°C). Light was not included in the thermodynamic calculations and, thus, the more positive the Gibbs free energy, the higher the photosynthetic energy requirement. Data and calculations are available upon request.

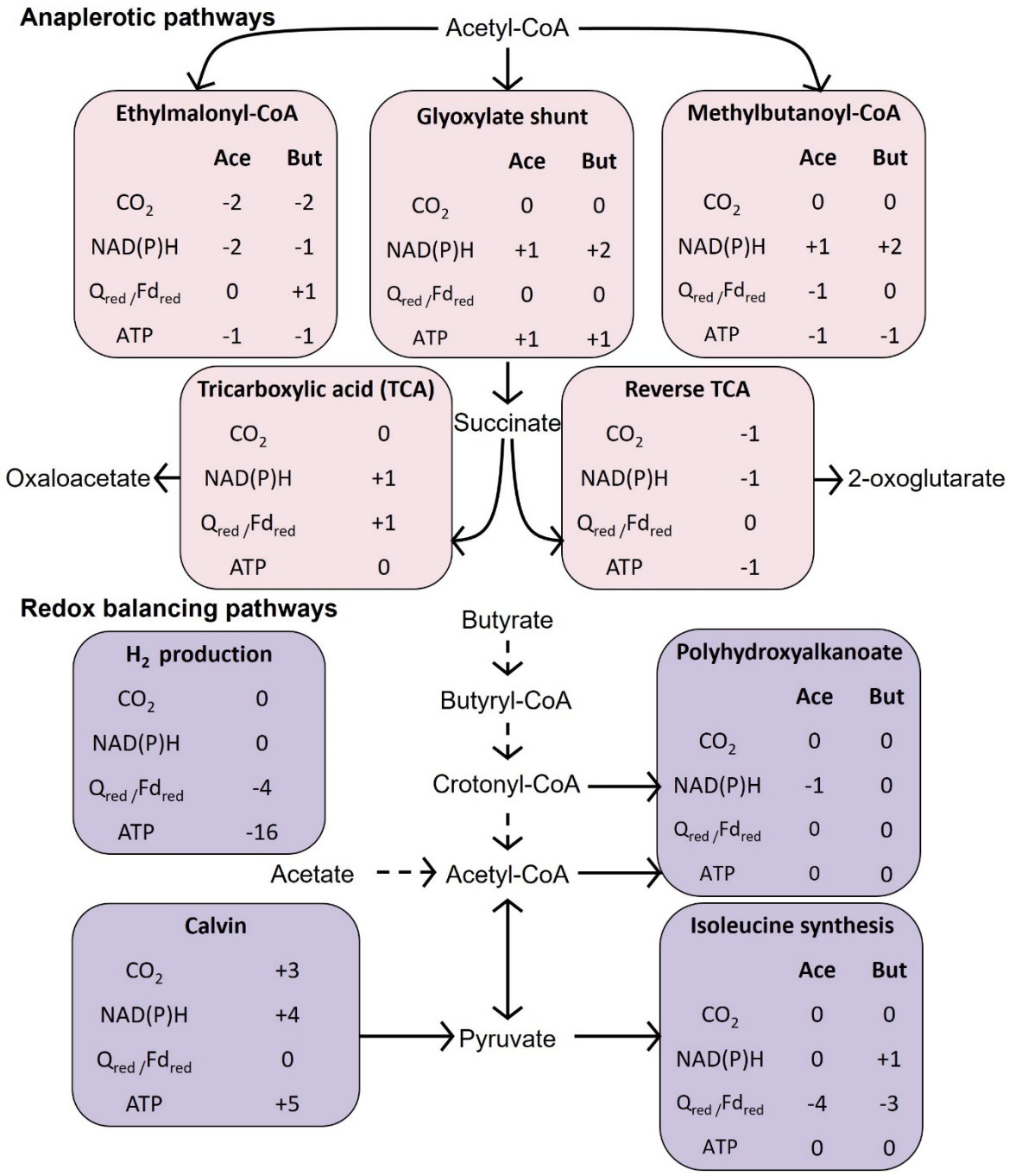

Figure 2 Redox and energy balance of key metabolic pathways involved in phototrophically grown purple bacteria

Net productions (+) or consumptions (-) of CO_2, reduced nicotinamide adenine dinucleotide (NAD), reduced quinone (Q_{red}) or ferredoxin (FD_{red}) and ATP for the main anaplerotic (pink) or redox balancing pathways (purple) based on reported enzymatic reactions (KEGG database). Acetate (Ace) and butyrate (But) were considered to account for the electron content of the carbon source. Succinate was used as a precursor for oxaloacetate and 2-oxoglutarate as it represents a common intermediate for acetate and butyrate assimilation. All calculations are

presented per mole of produced compound/monomer. Arrows: multi-reaction pathways; Dashed arrows: single-reaction.

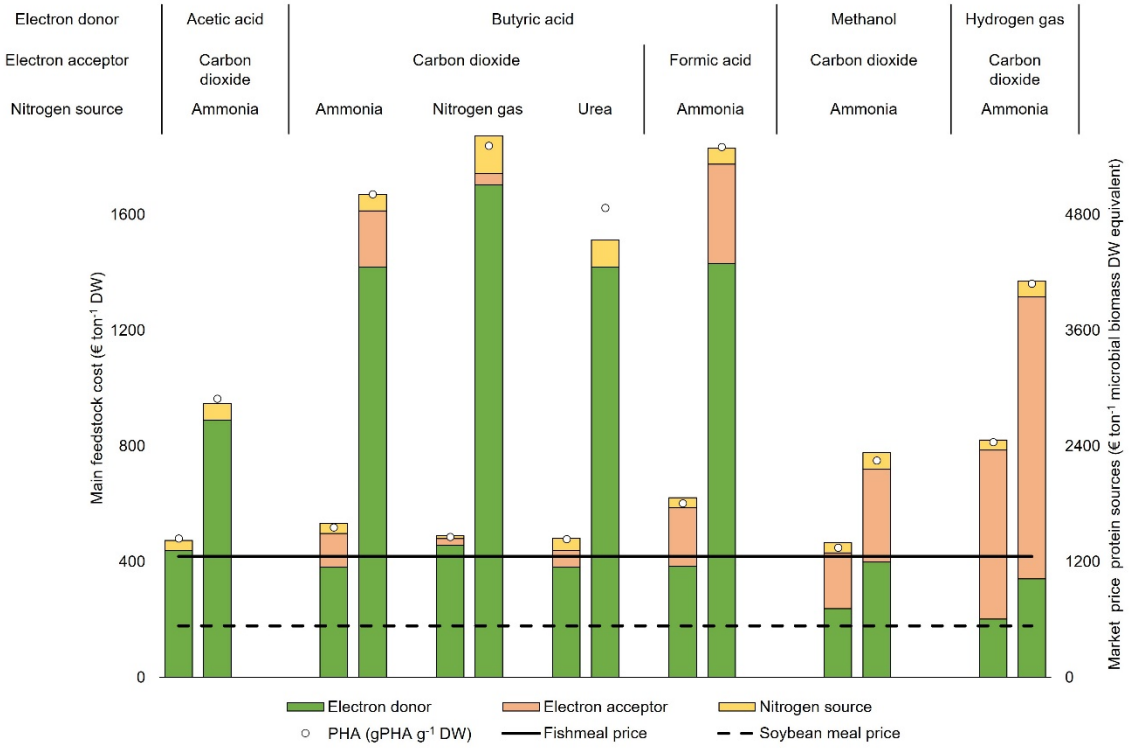

Figure 3 Main feedstock cost estimation for phototrophically grown purple bacteria

Main feedstock cost for phototrophic cultivation of purple bacteria on four electron donors, two electron acceptors and three nitrogen sources. Only carbon sources typically considered for industrial biotechnology applications were considered. Two scenarios were simulated: (i) biomass production without polyhydroxyalkanoate (PHA), and (ii) biomass production including 20% of the electrons stored as PHA. PHA was composed of 50% polyhydroxybutryate ($C_4H_6O_2$) and 50% polyhydroxyvalerate ($C_5H_8O_2$). A lower and higher cost estimation was simulated for each scenario to account for uncertainty. Cost of main feedstock for microbial biomass (0.65 kg protein kg^{-1} dry weight) was compared to recalculated market prices of two conventional protein sources namely, fishmeal (€1250 ton^{-1} product; €1250 ton^{-1} microbial biomass dry weight (DW) equivalent at 0.65 kg protein kg^{-1} product) and soybean meal (€410 ton^{-1} product; 530 ton^{-1} microbial biomass DW equivalent at 0.5 kg protein kg^{-1} product) [70]. Market price axis ranges a factor three above the cost axis, to reflect a typical industrial bulk product price/cost ratio. For the electron donors, current industrial prices of fossil counterparts were used.

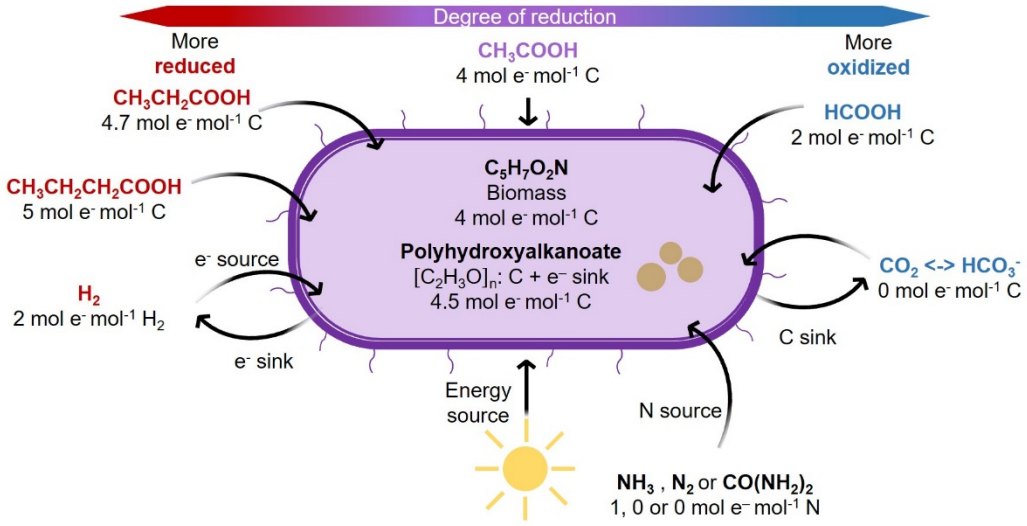

433

434 **Box 1, Figure I Redox homeostasis strategies for phototrophically grown purple bacteria**

435 Conceptual sketch of redox homeostasis strategies including CO_2 fixation, and production of
436 polyhydroxyalkanoates and H_2. A theoretical relative electron content for the carbon (C)
437 sources, nitrogen (N) sources and H_2 is given compared to the oxidized form CO_2. Values are
438 expressed in moles. The theoretical relative electron content for the carbon (C) sources,
439 nitrogen (N) sources and H_2 is expressed in moles. $CO(NH_2)_2$: urea.

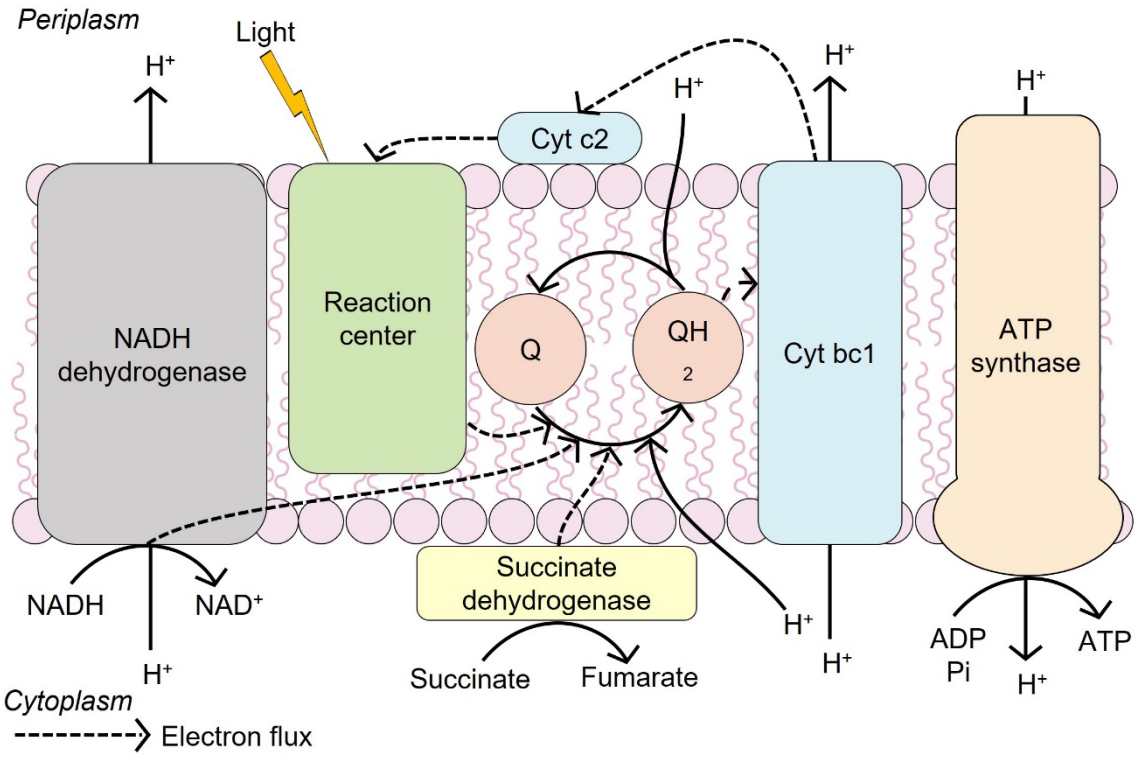

440

441 **BOX 3, Figure I Electron exchange for phototrophically grown purple bacteria**

Main intracellular membrane electrons exchange between the different actors involved in the photosynthesis and respiratory chain. Reduction of the quinone pool (Q/QH2) by the electron donor is represented by both the activity of succinate dehydrogenase (SDH) and NADH dehydrogenase. The conversion of light energy into chemical energy is represented by the cycling of electrons between the photosynthesis **reaction center**, the membranous pool of quinone (Q), the proton pumping cytochrome bc1 complex (Cyt bc1) and the soluble cytochrome c2 (Cyt c2). ATP is generated by ATP synthase using the produced proton gradient. Dashed arrows indicate the flow of electrons.

Text boxes

Box 1: Metabolic diversity and cyclic photophosphorylation of purple non-sulfur bacteria

Purple non-sulfur bacteria (PNSB) are a group of metabolically diverse alfa- and beta-Proteobacteria. To date, 28 genera and 95 species are known [1]. These microbes are characterized by their notable color, due to their pigmentation for energy capture from light. This enables them to grow phototrophically, using energy from light. Next to phototrophy, PNSB are also able to grow chemotropically in the dark, using oxygen as terminal electron acceptor [8,71]. Almost all PNSB can grow heterotrophically on acetate, however, other volatile fatty acids are also suitable. Organic acids, amino acids and carbohydrates can be metabolized as well. A few PNSB species are also able to grow on citrate or aromatic compounds. For autotrophic growth, PNSB rely on CO_2 as carbon source and either sulfate, iron or H_2 as electron donor. Apart from NH_3, most PNSB can also utilize dinitrogen or nitrogen containing organic molecules (amino acids...) as nitrogen source. Some PNSB are also able to assimilate nitrate [72].

When PNSB grow phototrophically, they perform cyclic photophosphorylation. In this type of metabolism, electrons excited by photons in the photosystem are transported through several electron carriers and recycled back to the photosystem. The photosynthetic reaction is in this case not providing reducing power as for oxygenic photosynthesis. During photoheterotrophic growth, electrons are thus obtained from external sources and notably from organic carbon. When a carbon source more reduced than the biomass is used, such as butyrate, PNSB have to oxidize the carbon source in an anabolic reaction. The reduced cofactors which are produced during this oxidizing anabolic reaction have to be recycled. When PNSB grow phototrophically, aerobic respiration cannot be used to reoxidize these cofactors. PNSB, therefore, have to exhibit several redox balancing strategies to dump the excess electrons and maintain redox homeostasis.

Box 2: Methodology stoichiometric and thermodynamic calculations

Stoichiometric calculations are based on the method described by Kleerebezem and Van Loosdrecht [15]. In short, the overall anabolic reaction (An) is divided into two half-reactions, namely the biomass synthesis reaction (An*) and an external electron donor (D) or acceptor (A) reaction, depending on the oxidation state of the carbon source (C), nitrogen source (N) and the biomass. To balance the reactions, coefficient Y_X^Z was included, with X referring to the reagent and Z referring to the type of reaction.

$$An^* = -Y_C^{An^*} * C - Y_N^{An^*} * N + 1 * C_1H_{1.4}O_{0.4}N_{0.2} + Y_{H2O}^{An^*} * H_2O + Y_{H^+}^{An^*} * H^+ + Y_{e^-}^{An^*} * e^-$$

$$An = An^* - Y_{e^-}^{An^*} / Y_{e^-}^{A} * A \text{ or } An = An^* - Y_{e^-}^{An^*} / Y_{e^-}^{D} * D$$

To illustrate this concept, an example is provided for the anabolic reaction of growth on butyrate as carbon source, NH_3 as nitrogen source and CO_2 as external electron acceptor.

$$An^* = -0.25\ CH_3(CH_2)_2COO^- - 0.2\ NH_3 + 1\ C_1H_{1.4}O_{0.4}N_{0.2} + 0.1\ H_2O + 0.75\ H^+ + 1\ e^-$$

$$\rightarrow Y_{e^-}^{An^*} = 1$$

$$A = -1\ CH_3(CH_2)_2COO^- - 6\ H_2O + 4\ CO_2 + 19\ H^+ + 20\ e^- \rightarrow Y_{e^-}^{A} = 20$$

$$An = -0.2\ CH_3(CH_2)_2COO^- - 0.2\ NH_3 - 0.2\ H^+ + 1\ C_1H_{1.4}O_{0.4}N_{0.2} + 0.4\ H_2O$$

For the thermodynamics, the Gibbs free energy for the reaction was calculated as described in Metcalf et al. [69]. Light was not included in the thermodynamic calculations and, thus, the more positive the Gibbs free energy, the higher the photosynthetic energy requirement. In short, the Gibbs free energy required to produce cell material (ΔG_S) is divided into three parts: (i) energy required to convert the carbon source to a pyruvate intermediate (ΔG_P), a frequent intermediate in the metabolism of microorganisms, (ii) energy to convert the pyruvate into cell material (ΔG_C), and (iii) energy required to reduce the nitrogen source to ammonia. These three factors are corrected with the efficiency of the captured energy (K), and m, equal to +1 if ΔG_P is positive and -1 if ΔG_P is negative.

$$\Delta G_S = \Delta G_P / K^m + \Delta G_C + \Delta G_N / K$$

Box 3: NAD^+ photoreduction and light-induced redox stress

Under phototrophic conditions, PNSB generate a proton motive force through electron cycling, which converts light energy to chemical energy in the form of reduced quinone and cytochrome bc1 complex (Box 3, Figure I) [73]. **Bacteriochlorophyll**, which is part of the reaction center, recovers its lost electron from reduced cytochrome c2. Under photoautotrophic conditions, with CO_2 as carbon source and H_2 as an electron donor, electrons obtained by membrane-bound uptake hydrogenase have been shown to flow through the quinone pool from H_2 to NAD^+ through the NADH dehydrogenase complex [74]. This reverse electron transfer to NAD^+, also called uphill electron transfer, allows the production of the redox poise required for CO_2 fixation. Under photoheterotrophic conditions, the carbon source also brings electrons required for biomass production. Electrons from the biomass can also be transferred to the quinone pool, notably through the membranous succinate dehydrogenase. Under illuminated conditions, it has been proposed that the NADH dehydrogenase complex is responsible for the oxidation of quinones through a mechanism relying on the light-driven **membrane potential** [74-76]. By modeling the electron transfer chain of *Rs. rubrum*, it was observed that higher light intensities,

induce a higher membrane potential (or high proton motive force), and a higher reverse electron flow to NAD^+ from the quinone pool. This leads to a more oxidized quinone and reduced nicotinamide cofactor pool [77]. We proposed that the NAD^+ photoreduction is responsible for the so-called light-induced redox stress which results from an overreduction of the NAD^+ cofactor pool. This light stress could occur upon a sudden light increase [13] or at the very beginning of a culture [21]. The sudden light increase supposedly triggered a higher flux of electrons toward the production of NADH thus blocking oxidative reaction necessary for cell metabolism.

References

1. Hallenbeck, P.C. (2017) *Modern topics in the phototrophic prokaryotes: Environmental and applied aspects* Springer

2. Capson-Tojo, G. *et al.* (2020) Purple phototrophic bacteria for resource recovery: Challenges and opportunities. *Biotechnol Adv*, 107567

3. Alloul, A. *et al.* (2021) Purple bacteria as added-value protein ingredient in shrimp feed: *Penaeus vannamei* growth performance, and tolerance against *Vibrio* and ammonia stress. *Aquaculture* 530, 735788

4. Wambacq, E. *et al.* (2022) Aerobes and phototrophs as microbial organic fertilizers: Exploring mineralization, fertilization and plant protection features. *Plos One* 17, e0262497

5. Hülsen, T. *et al.* (2016) Low temperature treatment of domestic wastewater by purple phototrophic bacteria: Performance, activity, and community. *Water Res* 100, 537-545. 10.1016/j.watres.2016.05.054

6. Blansaer, N. *et al.* (2022) Aggregation of purple bacteria in an upflow photobioreactor to facilitate solid/liquid separation: Impact of organic loading rate, hydraulic retention time and water composition. *Bioresource Technol* 348, 126806

7. Hülsen, T. *et al.* (2022) Outdoor demonstration-scale flat plate photobioreactor for resource recovery with purple phototrophic bacteria. *Water Res*, 118327

8. Alloul, A. *et al.* (2021) Cocultivating aerobic heterotrophs and purple bacteria for microbial protein in sequential photo-and chemotrophic reactors. *Bioresource Technol* 319, 124192

9. De Meur, Q. *et al.* (2018) Genetic plasticity and ethylmalonyl coenzyme A pathway during acetate assimilation in *Rhodospirillum rubrum* S1H under photoheterotrophic conditions. *Appl Environ Microb* 84,

10. Puyol, D. *et al.* (2017) A mechanistic model for anaerobic phototrophs in domestic wastewater applications: Photo-anaerobic model (PAnM). *Water Res* 116, 241-253. 10.1016/j.watres.2017.03.022

11. Cerruti, M. *et al.* (2020) Enrichment and aggregation of purple non-sulfur bacteria in a mixed-culture sequencing-batch photobioreactor for biological nutrient removal from wastewater. *Frontiers in Bioengineering and Biotechnology* 8. 10.3389/fbioe.2020.557234

12. Bayon-Vicente, G. *et al.* (2021) Analysis of the involvement of the isoleucine biosynthesis pathway in photoheterotrophic metabolism of *Rhodospirillum rubrum*. *Frontiers in Microbiology* 12,

13. Bayon-Vicente, G. *et al.* (2020) Global proteomic analysis reveals high light intensity adaptation strategies and polyhydroxyalkanoate production in *Rhodospirillum rubrum* cultivated with acetate as carbon source. *Frontiers in Microbiology* 11, 464

14. Montiel-Corona, V. and Buitrón, G. (2021) Polyhydroxyalkanoates from organic waste streams using purple non-sulfur bacteria. *Bioresource Technol* 323, 124610

15. Kleerebezem, R. and Van Loosdrecht, M.C. (2010) A generalized method for thermodynamic state analysis of environmental systems. *Critical Reviews in Environmental Science and Technology* 40, 1-54

16. Alloul, A. *et al.* (2018) Capture–ferment–upgrade: A three-step approach for the valorization of sewage organics as commodities. *Environ Sci Technol* 52, 6729-6742. 10.1021/acs.est.7b05712

17. Alloul, A. *et al.* (2019) Volatile fatty acids impacting phototrophic growth kinetics of purple bacteria: Paving the way for protein production on fermented wastewater. *Water Res* 152, 138-147

18. Alloul, A. *et al.* (2021) Unlocking the genomic potential of aerobes and phototrophs for the production of nutritious and palatable microbial food without arable land or fossil fuels. *Microbial Biotechnology*,

19. Spanoghe, J. *et al.* (2021) Microbial food from light, carbon dioxide and hydrogen gas: Kinetic, stoichiometric and nutritional potential of three purple bacteria. *Bioresource Technol* 337, 125364

20. Laguna, R. *et al.* (2011) Acetate-dependent photoheterotrophic growth and the differential requirement for the Calvin-Benson-Bassham reductive pentose phosphate cycle in Rhodobacter sphaeroides and Rhodopseudomonas palustris. *Arch Microbiol* 193, 151-154. 10.1007/s00203-010-0652-y

21. Leroy, B. *et al.* (2015) New insight into the photoheterotrophic growth of the isocytrate lyase-lacking purple bacterium Rhodospirillum rubrum on acetate. *Microbiology* 161, 1061-1072

22. Cerruti, M. *et al.* (2020) Effects of light/dark diel cycles on the photoorganoheterotrophic metabolism of Rhodopseudomonas palustris for differential electron allocation to PHAs and H2. *bioRxiv*,

23. Cabello Bergillos, F. (2008) *Cultivo en biorreactores de rhodospirillum rubrum en condiciones fotoheterotróficas* Universitat Autònoma de Barcelona

24. Linder, T. (2019) Making the case for edible microorganisms as an integral part of a more sustainable and resilient food production system. *Food Security*, 1-14

25. De Vrieze, J. *et al.* (2020) The hydrogen gas bio-based economy and the production of renewable building block chemicals, food and energy. *N Biotechnol* 55, 12-18

26. Stokes, J.E. and Hoare, D.S. (1969) Reductive pentose cycle and formate assimilation in *Rhodopseudomonas palustris*. *J Bacteriol* 100, 890-894

27. Wilson, S.M. *et al.* (2008) Identification of proteins involved in formaldehyde metabolism by *Rhodobacter sphaeroides*. *Microbiology (Reading, England)* 154, 296

28. Douthit, H.A. and Pfennig, N. (1976) Isolation and growth rates of methanol utilizing Rhodospirillaceae. *Arch Microbiol* 107, 233-234. 10.1007/BF00446847

29. Basak, N. *et al.* (2014) Photofermentative molecular biohydrogen production by purple-non-sulfur (PNS) bacteria in various modes: the present progress and future perspective. *Int J Hydrogen Energ* 39, 6853-6871

30. Cabecas Segura, P. *et al.* (2021) Effects of Mixing volatile fatty acids as carbon sources on *Rhodospirillum rubrum* carbon metabolism and redox balance mechanisms. *Microorganisms* 9, 1996

31. Sali, S. and Mackey, H.R. (2021) The application of purple non-sulfur bacteria for microbial mixed culture polyhydroxyalkanoates production. *Reviews in Environmental Science and Bio/Technology* 20, 959-983

32. Masepohl, B. (2017) Regulation of nitrogen fixation in photosynthetic purple nonsulfur bacteria. In *Modern topics in the phototrophic prokaryotes*, pp. 1-25, Springer

33. van Niel, C.B. and Muller, F. (1931) On the purple bacteria and their significance for the study of photosynthesis. *Recueil des travaux botaniques néerlandais* 28, 245-274

34. Hallenbeck, P.L. *et al.* (1990) Phosphoribulokinase activity and regulation of CO2 fixation critical for photosynthetic growth of *Rhodobacter sphaeroides*. *J Bacteriol* 172, 1749-1761

35. Falcone, D.L. and Tabita, F.R. (1993) Complementation analysis and regulation of CO_2 fixation gene expression in a ribulose 1, 5-bisphosphate carboxylase-oxygenase deletion strain of *Rhodospirillum rubrum*. *J Bacteriol* 175, 5066-5077

36. Erb, T.J. *et al.* (2007) Synthesis of C5-dicarboxylic acids from C2-units involving crotonyl-CoA carboxylase/reductase: the ethylmalonyl-CoA pathway. *Proceedings of the National Academy of Sciences* 104, 10631-10636

37. Erb, T.J. *et al.* (2010) The apparent malate synthase activity of *Rhodobacter sphaeroides* is due to two paralogous enzymes,(3 S)-malyl-coenzyme A (CoA)/β-methylmalyl-CoA lyase and (3 S)-malyl-CoA thioesterase. *J Bacteriol* 192, 1249-1258

38. Shimizu, T. *et al.* (2019) Introduction of glyoxylate bypass increases hydrogen gas yield from acetate and L-glutamate in *Rhodobacter sphaeroides*. *Appl Environ Microb* 85, e01873-01818

39. Gordon, G.C. and McKinlay, J.B. (2014) Calvin cycle mutants of photoheterotrophic purple nonsulfur bacteria fail to grow due to an electron imbalance rather than toxic metabolite accumulation. *J Bacteriol* 196, 1231-1237

40. Joshi, H.M. and Tabita, F.R. (1996) A global two component signal transduction system that integrates the control of photosynthesis, carbon dioxide assimilation, and nitrogen fixation. *Proceedings of the National Academy of Sciences* 93, 14515-14520

635 41. Tichi, M.A. and Tabita, F.R. (2000) Maintenance and control of redox poise in
636 *Rhodobacter capsulatus* strains deficient in the Calvin-Benson-Bassham pathway. *Arch*
637 *Microbiol* 174, 322-333

638 42. Hädicke, O. *et al.* (2011) Metabolic network modeling of redox balancing and
639 biohydrogen production in purple nonsulfur bacteria. *BMC systems biology* 5, 1-18

640 43. Hauf, W. *et al.* (2013) Metabolic changes in *Synechocystis* PCC6803 upon nitrogen-
641 starvation: excess NADPH sustains polyhydroxybutyrate accumulation. *Metabolites* 3,
642 101-118

643 44. Brandl, H. *et al.* (1991) The accumulation of poly (3-hydroxyalkanoates) in
644 Rhodobacter sphaeroides. *Arch Microbiol* 155, 337-340

645 45. Cabecas Segura, P. *et al.* (2022) Study of the production of poly (hydroxybutyrate-co-
646 hydroxyhexanoate) and poly (hydroxybutyrate-co-hydroxyvalerate-co-hydroxy
647 hexanoate) in *Rhodospirillum rubrum*. *Appl Environ Microb*, AEM. 01586-01521

648 46. Bayon-Vicente, G. *et al.* (2020) Photoheterotrophic assimilation of valerate and
649 associated polyhydroxyalkanoate production by *Rhodospirillum rubrum*. *Appl Environ*
650 *Microb* 86, e00901-00920

651 47. De Meur, Q. *et al.* (2020) New perspectives on butyrate assimilation in *Rhodospirillum*
652 *rubrum* S1H under photoheterotrophic conditions. *BMC microbiology* 20, 1-20

653 48. Joshi, H.M. and Tabita, F.R. (2000) Induction of carbon monoxide dehydrogenase to
654 facilitate redox balancing in a ribulose bisphosphate carboxylase/oxygenase-deficient
655 mutant strain of *Rhodospirillum rubrum*. *Arch Microbiol* 173, 193-199

656 49. McCully, A.L. *et al.* (2020) Reductive tricarboxylic acid cycle enzymes and reductive
657 amino acid synthesis pathways contribute to electron balance in a *Rhodospirillum*
658 *rubrum* Calvin-cycle mutant. *Microbiology* 166, 199-211

659 50. Richardson, D.J. *et al.* (1988) The role of auxiliary oxidants in maintaining redox
660 balance during phototrophic growth of *Rhodobacter capsulatus* on propionate or
661 butyrate. *Arch Microbiol* 150, 131-137

662 51. Sajitz, P. *et al.* (1993) Isolation and properties of trimethylamine N-
663 oxide/dimethylsulfoxide reductase from the purple bacterium Rhodospirillum rubrum.
664 *Zeitschrift für Naturforschung C* 48, 812-814

665 52. Rizk, M.L. *et al.* (2011) Redox homeostasis phenotypes in RubisCO-deficient
666 Rhodobacter sphaeroides via ensemble modeling. *Biotechnology progress* 27, 15-22

667 53. Hartsock, A. and Shapleigh, J.P. (2011) Physiological roles for two periplasmic nitrate
668 reductases in *Rhodobacter sphaeroides* 2.4. 3 (ATCC 17025). *J Bacteriol* 193, 6483-
669 6489

670 54. Siefert, E. and Pfennig, N. (1979) Chemoautotrophic growth of *Rhodopseudomonas*
671 species with hydrogen and chemotrophic utilization of methanol and formate. *Arch*
672 *Microbiol* 122, 177-182

673 55. Quayle, J. and Pfennig, N. (1975) Utilization of methanol by Rhodospirillaceae. *Arch*
674 *Microbiol* 102, 193-198

675 56. Fradinho, J. *et al.* (2014) Photosynthetic mixed culture polyhydroxyalkanoate (PHA)
676 production from individual and mixed volatile fatty acids (VFAs): Substrate
677 preferences and co-substrate uptake. *J Biotechnol* 185, 19-27.
678 10.1016/j.jbiotec.2014.05.035

679 57. Eady, R.R. (1996) Structure− function relationships of alternative nitrogenases.
680 *Chemical reviews* 96, 3013-3030

681 58. Luxem, K.E. *et al.* (2022) Carbon substrate re-orders relative growth of a bacterium
682 using Mo-, V-, or Fe-nitrogenase for nitrogen fixation. *Environ Microbiol* 24, 2170-
683 2176

684 59. Machado, D. *et al.* (2018) Fast automated reconstruction of genome-scale metabolic
685 models for microbial species and communities. *Nucleic Acids Res* 46, 7542-7553

686 60. Chowdhury, N.B. *et al.* (2022) Characterizing the interplay of rubisco and nitrogenase
687 enzymes in anaerobic-photoheterotrophically grown Rhodopseudomonas palustris
688 CGA009 through a genome-scale metabolic and expression model. *bioRxiv*,

689 61. Alsiyabi, A. *et al.* (2019) Modeling the interplay between photosynthesis, CO2 fixation,
690 and the quinone pool in a purple non-sulfur bacterium. *Sci Rep-Uk* 9, 1-9

691 62. Alsiyabi, A. *et al.* (2021) Synergistic experimental and computational approach
692 identifies novel strategies for polyhydroxybutyrate overproduction. *Metabolic*
693 *Engineering* 68, 1-13

694 63. Delamare-Debouteville, J. *et al.* (2019) Mixed culture purple phototrophic bacteria is
695 an effective fishmeal replacement in aquaculture. *Water Research X* 4, 100031

696 64. Alloul, A. *et al.* (2021) Operational strategies to selectively produce purple bacteria for
697 microbial protein in raceway reactors. *Environ Sci Technol*. 10.1021/acs.est.0c08204

698 65. Fernández, F.A. *et al.* (2019) Costs analysis of microalgae production. In *Biofuels from*
699 *algae*, pp. 551-566, Elsevier

700 66. Oostlander, P. *et al.* (2020) Microalgae production cost in aquaculture hatcheries.
701 *Aquaculture* 525, 735310

702 67. Tan, D. *et al.* (2021) Grand challenges for industrializing polyhydroxyalkanoates
703 (PHAs). *Trends Biotechnol* 39, 953-963

704 68. Kayfeci, M. *et al.* (2019) Hydrogen production. In *Solar hydrogen production*, pp. 45-
705 83, Elsevier

706 69. Metcalf *et al.* (2014) *Wastewater engineering: treatment and resource recovery*
707 McGraw Hill Education

708 70. IndexMundi (2022). Commodity prices.

71. Blankenship, R.E. (2010) Early evolution of photosynthesis. *Plant physiology* 154, 434-438

72. Imhoff, J.F. (2006) The phototrophic alpha-proteobacteria. In *The Prokaryotes* (Dworkin, M. *et al.*, eds), pp. 41-64, Springer-Verlag

73. Hunter, C.N. *et al.*, eds (2008) *The purple phototrophic bacteria* (Vol. 28, Springer

74. Herter, S.M. *et al.* (1998) Complex I of *Rhodobacter capsulatus* and its role in reverted electron transport. *Arch Microbiol* 169, 98-105

75. Tichi, M.A. *et al.* (2001) Complex I and its involvement in redox homeostasis and carbon and nitrogen metabolism in *Rhodobacter capsulatus*. *J Bacteriol* 183, 7285-7294

76. Verméglio, A. and Joliot, P. (2014) Modulation of the redox state of quinones by light in *Rhodobacter sphaeroides* under anaerobic conditions. *Photosynth Res* 120, 237-246

77. Klamt, S. *et al.* (2008) Modeling the electron transport chain of purple non-sulfur bacteria. *Molecular systems biology* 4, 156